Impact of wildfire on ^{137}Cs and ^{90}Sr wash-off in heavily contaminated forests in the Chernobyl exclusion zone[☆]

Yasunori Igarashi [a], Yuichi Onda [b, *], Yoshifumi Wakiyama [a], Alexei Konoplev [a], Mark Zheleznyak [a], Hlib Lisovyi [c], Gennady Laptev [c], Volodyill Damiyanovich [d], Dmitry Samoilov [d], Kenji Nanba [a], Serhii Kirieiev [d]

[a] Institute of Environmental Radioactivity, Fukushima University, 1 Kanayagawa, Fukushima, 960-1296, Fukushima, Japan
[b] Center for Research in Isotopes and Environmental Dynamics, University of Tsukuba, Tsukuba, Ibaraki, 305-8572, Japan
[c] Ukrainian Hydrometeorological Institute, Kiev, 03028, Ukraine
[d] Chernobyl Ecocentre, State Agency of Ukraine on Exclusion Zone Management, Chernobyl, 07270, Ukraine

ARTICLE INFO

ABSTRACT

Wildfires may play a role in redistributing radionuclides in the environment in combination with hydrological processes such as surface runoff and soil erosion. We investigated plot-scale radionuclide wash-off at forest sites affected by wildfires in the Chernobyl Exclusion Zone (CEZ). We also compared speciation of the washed-off radionuclides with those in previous studies conducted just after the accident in 1986. We observed the surface runoff and the radionuclide wash-off with a soil erosion plot at forest and post-fire sites during May–September 2018. In the post-fire site, 2.81 mm of surface runoff was observed in at least three flow events resulting from 285.8 mm total rainfall. The fluxes of dissolved and particulate ^{137}Cs were estimated as 4.9 and 161 Bq m^{-2}, respectively. The dissolved phase ^{90}Sr flux was estimated as 214 Bq m^{-2}. At the forest site, a single surface runoff (0.67 mm) event was generated by rainfall of 182.2 mm. The fluxes of dissolved and particulate ^{137}Cs wash-off values were 6.2 and 8.6 Bq m^{-2}, respectively. The flux of dissolved ^{90}Sr wash-off from the forest was estimated as 45.1 Bq m^{-2}. The distribution coefficient, which indicates the dissolved-particulate form of radionuclides, in the post-fire site was 30 times higher than that in the forest site, indicating the importance of particulate ^{137}Cs wash-off after fire in the CEZ. The entrainment coefficients for dissolved and particulate ^{137}Cs concentrations were around 50 times lower than those obtained in the corresponding position within the CEZ immediately after the accident in 1987. The effect of downward migration of ^{137}Cs over 30 years led to decreased entrainment coefficients for dissolved and particulate ^{137}Cs. The effect of downward migration of radionuclides was considered sufficient to indicate changes in normalized liquid and solid radionuclides wash-off entrainment coefficient and the distribution coefficient in this study.

1. Introduction

During and after the Chernobyl nuclear power plant (CNPP) accident in April 1986, a huge number of radionuclides were released into the environment (Smith and Beresford, 2005). Redistribution of long-lived radionuclides, such as ^{137}Cs and ^{90}Sr, from the contaminated area has been of great concern in terms of the radiological risks for residents in the downstream area (IAEA, 2006). Dissolved and particulate radionuclide wash-offs, which are associated with water movement and sediment transport, are important processes determining quantities of redistributions of the radionuclides (e.g., Garcia-Sanchez and Konoplev, 2009; Yoshimura et al., 2015a; Wakiyama et al., 2019). In July 2016, a severe wildfire occurred near the CNPP in the Chernobyl Exclusion Zone (CEZ) (Fig. 1A and B). The area is known as "Red Forest" (RF), and remains one of the most radionuclide-contaminated terrestrial ecosystems on Earth (Nepyivoda, 2005). Wildfire may play a role in redistributing radionuclides in the environment in combination with hydrological processes such as surface runoff and soil erosion.

Large-scale observations of plot scale radionuclide wash-off from contaminated areas revealed the importance of speciation of
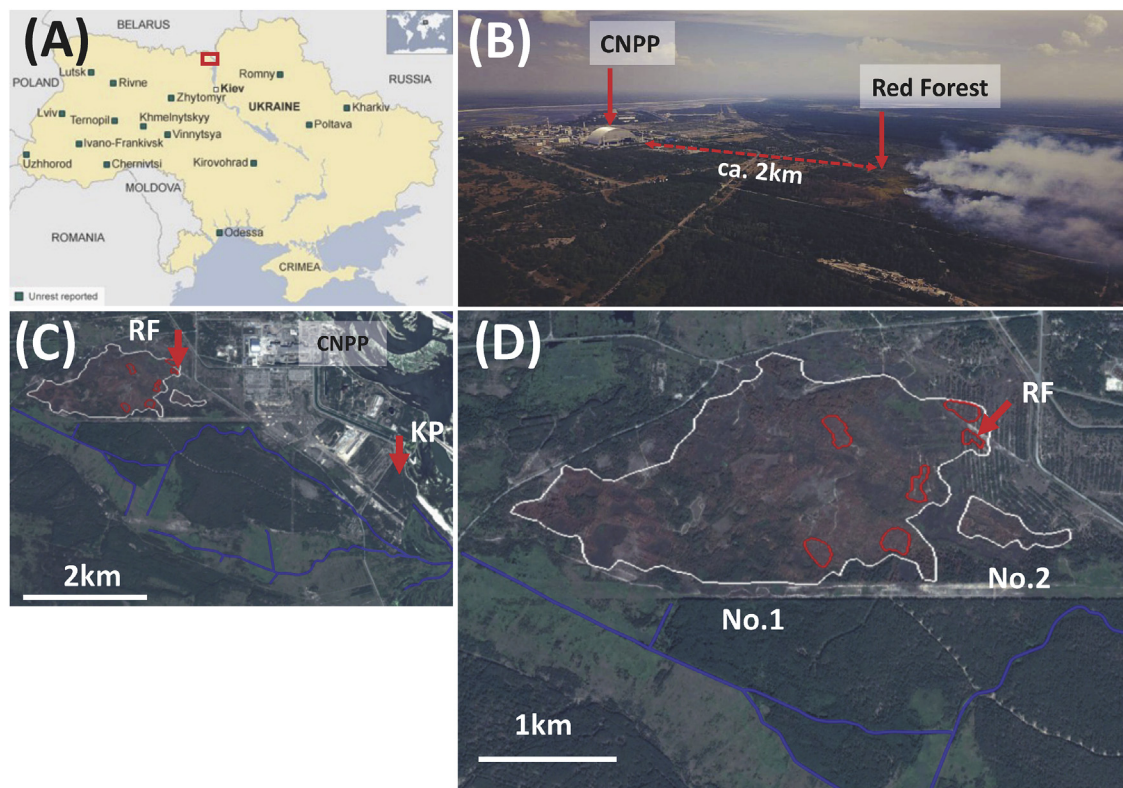
Fig. 1. Wildfire events in 2016. The Red Forest site was burned by a wildfire on July 15−18, 2016 (A). White and red outlined areas show the low- and high-severity fire areas, respectively (B). The event on July 15−18 (No. 1) affected grass and pine trees. The event on July 29−30 (No. 2) affected grasses and small trees (bushes). (For interpretation of the references to colour in this figure legend, the reader is referred to the Web version of this article.)

radionuclides in soil and water bodies (Konoplev and Bulgakov, 1995; Konoplev et al., 1996; Bulgakov et al., 1999; Konoplev and Bulgakov, 1999; Konoplev and Bulgakov, 2000a; Konoplev and Bulgakov, 2000b). These investigations contributed to establishment of model parameterization schemes (Konoplev et al., 1992), and the assessment of transfer factors between the dissolved and particulate phases of radionuclides in the environment (Garcia-Sanchez et al., 2005; Garcia-Sanchez and Konoplev, 2009). Such studies indicated that the mobility of radionuclides of accidental origin is governed by its chemical forms in fallout deposits and also the post-fallout environment. Rates of leaching, fixation-remobilization, and sorption-desorption of the mobile fraction (its dissolved-particulate distribution) are determined by the environmental characteristics (Konoplev et al., 1992; Konoplev and Bulgakov, 1995). In particular, radiocesium is known to be highly selective, reversible sorption and fixation, and can strongly bind to soil and sediment particles containing micaceous clay minerals in the environment (Konoplev and Bulgakov, 1999).

After the Fukushima nuclear power plant accident in 2011, it was found that soil and sediment transport played an important role in ^{137}Cs dynamics. For instance, ^{137}Cs, which was hydrologically transported in the terrestrial environment, was mainly found in a particulate form in the Fukushima region (e.g. Yoshimura et al., 2015b; Evrard et al., 2015; Konoplev et al., 2016; Iwagami et al., 2017). Yamashiki et al. (2014) estimated that 84%−92% of the total ^{137}Cs transported in a basin's fluvial system in Fukushima was carried in particulate form. The large proportion of the particulate fraction has also been reported for the other water system in Fukushima (e.g. Nagao et al., 2013; Sakaguchi et al., 2015; Yoshimura et al., 2015b). It is also known that a large proportion of the particulate form (solid ^{137}Cs) is associated with the clay fraction

in the soils and sediments of the Fukushima area, which accordingly has a high radiocesium interception potential (Nakao et al., 2012, 2014; Uematsu et al., 2015; Konoplev et al., 2016). A comparison study between Chernobyl and Fukushima revealed that regional differences such as soil type and annual precipitation could result in differences in radionuclide dynamics (Konoplev et al., 2016). Such differences include the decrease of radionuclides at the surface by their vertical downward migration in soil (Konoplev et al., 1992) and the reduced radionuclide mobilities over time due to their fixation to soil/sediment particles (Konoplev et al., 1992; Konoplev and Bulgakov, 1995). Thus, dissolved and particulate radionuclide dynamics are crucial for understanding the redistribution in the environment, and the radionuclide form in the soil plays an important role in dissolved and particulate radionuclide dynamics.

Wildfire is a primary natural disaster agent affecting the structure and composition of many forest ecosystems. It has been considered that the radionuclides in the environment surrounding the CEZ could be redistributed by wildfires (Yoschenko et al., 2006, 2009). After a wildfire, hydrological processes, such as surface runoff and erosion, can change drastically at the slope scale (Debano and Krammes, 1966). This is because the combusted organic compounds produced by the heat generated by the fire are cooled and the rain particles form a water repellent coating on the soil particles (Debano and Krammes, 1966; Debano et al., 1967; Huffman et al., 2001). Wildfire is reported to induce soil water repellency and reduce water permeability (e.g., Scott and Van Wyk, 1990; Moody et al., 2013). Furthermore, after forest fires, outdoor observations have revealed that the runoff rate and the runoff peak also increase (e.g., Scott and Van Wyk, 1990; Shahlaee et al., 1991; Imeson et al., 1992; Kutiel et al., 1995; Inbar et al., 1998; Robichaud,

2003). Debano et al. (1967) indicated that the surface flow occurs after the ash layer that is formed on the water repellent soil becomes saturated. Furthermore, current studies (e.g., Mills and Fey, 2004; Onda et al., 2008) described the influence of the crust formed on the soil surface, and showed that the surface flow generation mechanism evolved with the change of the soil surface on a soil surface that had experienced wildfires. At an early stage, a saturation overland flow is generated on the surface of the ash, and subsurface storm flow is generated immediately above the water repellent soil after penetrating the surface ash, which has relatively high permeability. This pattern causes surface wash-off. It has been stated that Horton overland flow occurs because the ash layer is compressed when the runoff occurs, and it becomes difficult for rain to penetrate when a crust is formed (Onda et al., 2008). These studies suggest the occurrence of wildfire is important not only in re-scattering the radionuclides contained in vegetation into the air, but also in sediment transport phenomena associated with the occurrence of surface flow.

The goal of this study, therefore, was to report the impact of wildfires on the surface runoff, and the effects of changes in radionuclide speciation in the environment after 30 years on dissolved and particulate wash-off of radionuclides in the CEZ. To meet this aim, we conducted Universal Soil Loss Equation (USLE; Wischmeier and Smith, 1978) plot measurements at a post-fire and an undisturbed forest site in the CEZ in the summer of 2018. It is envisaged that the comparison between post-fire and undisturbed forest thereby assisting the further understanding of wildfires impact for redistributing radionuclides in the environment in combination with hydrological processes such as surface runoff and soil erosion.

2. Material and methods

2.1. Study site

Our field observations were carried out in the CEZ, Ukraine (Fig. 1A). Post-fire, known as "Red Forest" (RF), and forest undisturbed by wildfire in Kopachi (KP) sites were selected (Fig. 1B). In 1987, in the course of clean-up works radioactive materials (topsoil and contaminated tree trunks from the dead pines of the RF killed by extreme radiation levels in 1986), had been reclaimed in-situ in trenches a few meters deep (cf. Arkhipov et al., 1994; Bugai et al., 2002). The current pine trees in RF was established above the disposal trenches. Thus, the area remains one of the most radioactive contaminated terrestrial ecosystems on Earth (Nepyivoda, 2005). The KP site is not inside the "Red Forest" but was also highly contaminated. The first wildfire event in 2016 lasted from July 15 to July 18 (Area No.1 in Fig. 1D) around the RF. The burned area was about 2 km from the CNPP (Fig. 1B). The second forest fire was also occurred from July 29 to July 30 (Area No.2 in Fig. 1D) around the RF. The second forest fire affected grasses and small trees (bushes). The burned area was classified into two categories: (1) low-fire-severity, which contains the grasses and small trees (bush) (white solid area; in Figs. 1C and D) and (2) high-fire-severity, which contains the grasses and tree vegetation (red solid area; in Fig. 1C and D). The low- and high-severity areas were estimated as 2.51 and 0.10 km^2, respectively.

The plots (5 m × 22.13 m) were installed in the RF (Fig. 2 A1 and A2) and KP (Fig. 2 B1 and B2) sites at end of November 2017. The forest ecosystem at the RF site had completely mortality as a result of the severe wildfire event in 2016. The plot at the RF site was located on the 3.6% slope. The RF site contained an artificial pine forest before the wildfire event in 2016. Tree height and tree density in 2009 were about ~12 m and 800–1500 trees ha^{-1}, respectively. The plot was installed on a 6.2% slope at the mature pine

forest at the KP site. The current ^{137}Cs and ^{90}Sr inventory in RF were estimated as 113800 and 12700 kBq m^{-2}, respectively (Table 1), from the soil samples. The details of soil samples are available in Section 2.2. The current ^{137}Cs and ^{90}Sr inventory in KP were estimated as 8700 and 6300 kBq m^{-2}, respectively. It should be noted that the inventories at the RF site were calculated for a profile of 0−1 m soil depth. As mentioned above, contaminated tree trunks had been reclaimed in trenches a few meters deep at the RF site (cf. Arkhipov et al., 1994; Bugai et al., 2002). Thus, ^{137}Cs and ^{90}Sr could be assumed to be present in the artificial deeper layer. In this study, therefore, the RF inventory was defined as ^{137}Cs and ^{90}Sr concentration up to 1 m depth. In contrast, the vertical profile of ^{137}Cs and ^{90}Sr concentration in soil at the KP enabled us to confirm that 1-m depth soil samples were sufficient for inventory estimation.

Rainfall was monitored using a tipping bucket rain gauge (Model RG3-M, HOBO Computer, Bourne, MA, USA) beside the USLE plot in each site. Surface runoff and eroded soil were trapped in plastic tanks (total volume of 370 L by 3-prstic tanks; Fig. 2. A2 and B2). During the summer field campaign in 2018, discharge from the plots was monitored using a triangular weir with a water gauge (WT-HR 500, TruTrack Inc., Christchurch, New Zealand) set up at the outlet of each plot. We also measured the total runoff volumes by weight. Eroded sediments in each tank were collected for weighing and radionuclide measurement at the laboratory as explained in Section 2.2.

The Rainfall erosivity factor (R) estimates rainfall erosivity as a combined function of event frequency, intensity, and rainfall amount. The R factor for each rain-fall event, which is a product of the kinetic energy of an event (E) and its maximum 30 min intensity (I_{30}) (Renard and Freimund, 1994; Laceby et al., 2016) was calculated as follows:

$$R = \sum_{i=1}^{n} EI_{30} \tag{1}$$

where R equals the average rainfall erosivity (MJ mm ha^{-1} h^{-1}) in a given period, n is the number of the period of data utilized, and EI_{30} was calculated as

$$EI_{30} = \frac{1}{n} \left(\sum_{r=1}^{o} e_r v_r \right) I_{30} \tag{2}$$

where e_r is the rainfall energy per unit depth of rainfall (MJ ha^{-1} mm^{-1}), v_r is the volume of rainfall (mm) during the given time interval r, and I_{30} is the maximum rainfall intensity over a 30-min period within the rainfall event (mm h^{-1}). For each time interval, e_r was calculated as

$$e_r = 0.29[1 - 0.72 \exp(-0.05 i_r)] \tag{3}$$

where i_r is the rainfall intensity (mm h^{-1}) (Renard and Freimund, 1994).

2.2. Field sampling and laboratory analysis

The run-off samples collected in receiving tanks were transferred to clean canisters, making sure all the particulate sediments were picked up, then weighed. No filtration and preservation of the samples was made upon collection. Samples were transported to the laboratory at the Ukrainian Hydrometeorological Institute (UHMI) in Kiev, and stored in a dark place prior to further processing. We also measured pH and electrical conductivity of the sampled solution at the field and the laboratory, and confirmed that there were no drastic chemical changes in solution caused by
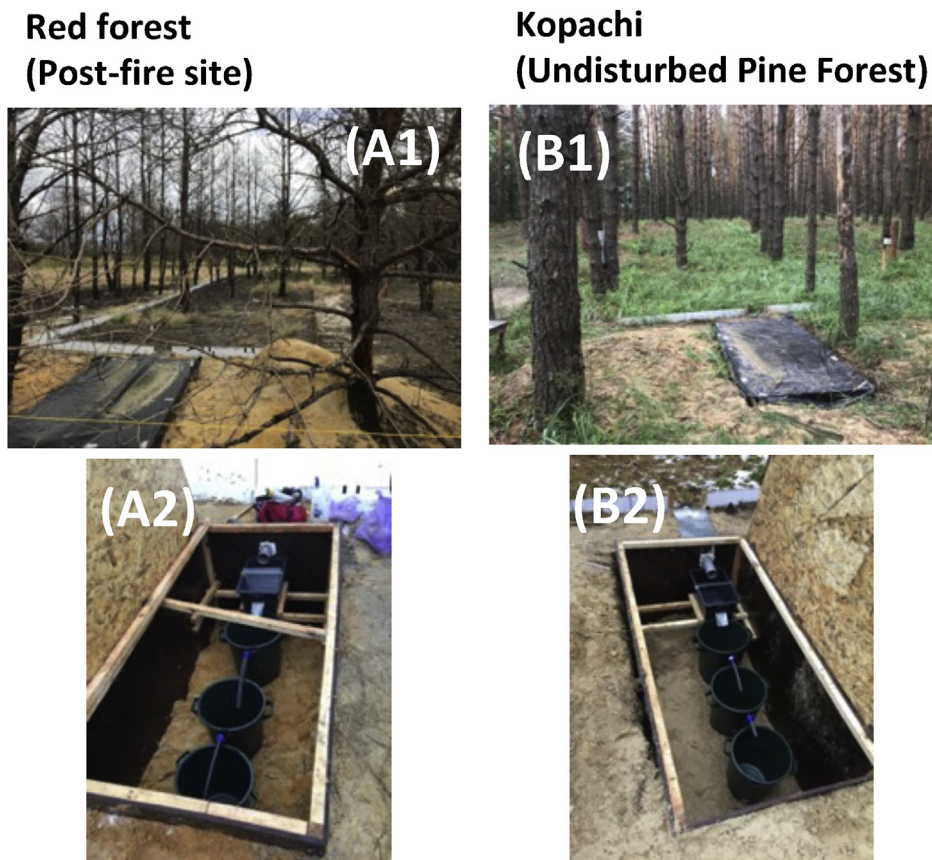
Red forest (Post-fire site)

Kopachi (Undisturbed Pine Forest)

Fig. 2. Pictures of the plots and the tank system designed to trap eroded soil (taken in April 2018).

Table 1
Characteristics of the study plots.

Site	Vegetation type	Slope	^{137}Cs inventory	^{90}Sr inventory	Radionuclide concentrations at the surface		
					Soil layer	Mean ^{137}Cs concentration	Mean ^{90}Sr concentration
		(%)	(MBq m^{-2})	(MBq m^{-2})		(kBq kg^{-1})	(kBq kg^{-1})
Red forest	Post-fire (pine forest)	3.6	113.8 [a]	12.7 [a]	Ash	1.7	796.7
					Soil ($h = 0-1$ cm)	2.9	182.3
					Soil ($h = 1-2$ cm)	2.1	57.1
					Soil ($h = 1-3$ cm)	9.2	4.0
Kopachi	Pine forest	6.2	8.7	6.3	Litter	0.2	3.3×10^{-2}
					Soil ($h = 0-1$ cm)	2.1	1.4×10^{-2}
					Soil ($h = 1-2$ cm)	6.3	0.4×10^{-2}
					Soil ($h = 1-3$ cm)	9.1	0.3×10^{-2}

[a] The inventory was estimated for soil core samples from 0 to 1 m soil depth.

sample transport.

At the laboratory, the physico-chemical parameters were measured again to check the samples or correct errors made in the field. After the sediment particles had settled to the bottom of the canister, the liquid phase (LP) was decanted to another clean canister and the particulate concentrate (SS) was transferred to the NALGENE centrifuge tube for separation of sediment from supernatant (Sigma 3 M, 3000 rpm, 5 min). After centrifugation, the SS samples were freeze-dried (Labconco 6 L), weighed, and prepared for gamma-spectrometric measurements. The decanted LP of the

run-off samples were filtered in a vacuum operated in-line filtration unit equipped with a "sandwich" type combined filter (Petryanov's FFP-15-1.5 prefilter + Blue Ribbon Grade paper filter) followed by a final filtration in a 0.45-μm membrane filter (Millipore Omnipore, Germany). Depending on the level of measurable concentration, gamma measurements were performed either directly using a 0.5-L Marinelli beaker, or after prior concentration of radionuclides on a cartridge filled with the radiocesium selective sorbent (ANFEZH®, EKSORB Ltd., Russia). Filters and sorbent were dried at 105 °C overnight to a constant weight, thoroughly mixed if

necessary, and packed in a container for gamma-spectrometry analysis.

The ^{137}Cs content was measured by direct gamma-ray spectrometry using a low-background HPGe detector GMX40C (ORTEC, USA). The efficiency of the detector was calibrated following the measurements of certified reference materials by the National Institute of Standards and Technology (NIST; MD, USA), International Atomic Energy Agency (IAEA; Vienna, Austria), and the National Physical Laboratory (NPL; Middlesex, UK) for various mass values and filling depth of containers. Measuring time was optimized (controlled by operator) to ensure that the statistical error in the peak of interest (for example, ^{137}Cs at 662 keV) did exceed 0.15 at the 1-sigma confidence level. The activity of gamma-emitting radioisotopes was calculated using GammaVision 5.1 and the ErlLib suite (Liverpool University, UK) adopted at UHMI. No significant statistical differences between the results of either calculation were encountered.

The ^{90}Sr was determined after preconcentration using carbonate/hydroxide precipitation followed by serial extraction chromatography on Sr-resin (Eichrom, USA) and measurements of separated radionuclide on liquid scintillation counting controlling the building-up of the equilibrium ^{90}Sr/^{90}Y (TriCarb 2900 TR, PerkinElmer, USA). To quantify ^{137}Cs and ^{90}Sr contamination, soil cores were collected with a 30-cm linear core sampler DIK-110C (DAIKI, Japan) with a 5-cm-diameter plastic cylinder. The ^{137}Cs and ^{90}Sr measurement of collected samples were also measured as mentioned above.

2.3. Calculation of radionuclide wash-off parameters

The dissolved and particulate radionuclide activity concentration in the wash-off depended on the radionuclide inventory at each site. We used the following parameters to provide an easy comparison. The normalized "liquid" (dissolved) and "solid" (particulate) wash-off coefficient at a given time in dissolved (L_c; m^{-1}) and particulate (S_c; m^2 g^{-1}) were defined as follows:

$$L_c(t) = \frac{C_w(t)}{C_s(t)} \tag{4}$$

$$S_c(t) = \frac{C_a(t)}{C_s(t)} \tag{5}$$

where C_w and C_a are the radionuclide concentration in solution (Bq L^{-1}) and radionuclide concentration on suspended particles (Bq kg^{-1}), respectively, for a given t (sample time); and C_s is the inventory of the radionuclides (Bq m^2), not the initial deposition.

We also defined the normalized liquid and solid radionuclides (as defined above; N_l and N_s, respectively) wash-off entrainment coefficient (L_c (m^{-1}) and S_c (m^2 g^{-1}), respectively), which were weighted-mean parameters during the given period (Bulgakov et al., 1991; Konoplev et al., 1992; Bulgakov et al., 1999; Garcia-Sanchez et al., 2005; Konoplev et al., 2016) as follows:

$$N_l = \frac{1}{C_s} \frac{\int_0^T C_w(t)Q_w(t)dt}{\int_0^T Q_w(t)dt} = \frac{\overline{C_w}}{C_s(t)} \tag{6}$$

$$N_s = \frac{1}{C_s} \frac{\int_0^T C_a(t)Q_S(t)dt}{\int_0^T Q_S(t)dt} = \frac{\overline{C_a}}{C_s(t)} \tag{7}$$

where $\overline{C_w}$ is the weighted-mean radionuclide concentration in solution (Bq L^{-1}); $\overline{C_a}$ is the weightedmean radionuclide concentration on suspended particles (Bq kg^{-1}); and Q_w and Q_S are the flow rate of water and suspended materials for a given time t, respectively.

Radionuclide exchanges between dissolved and particulate phases of soil−water systems are characterized by the distribution coefficient K_d (L kg^{-1}), which is calculated by dividing particulate radionuclide concentrations by the dissolved radionuclide concentration (e.g., Konoplev et al., 1992; Garcia-Sanchez et al., 2005; Konoplev et al., 2016) as follows:

$$K_d = \frac{\overline{C_w}}{\overline{C_a}} \tag{8}$$

3. Results and discussion

3.1. Event-based surface wash-off and radionuclide concentrations

In Table 2, the surface flow and the rainfall were observed during May and September of 2018. The sediments contained in the surface flow and the radionuclide contents in dissolved and particulate states were also showed. From May to September 2018, four timed filed observations were made on May 21, July 2, July 30, and September 26. During this period, only one outflow event was observed at least three times from June 12 to July 28 at the RF site and June 30 at the KP site.

At the RF site, because of the rainfall events that occurred on June 12 and June 30 there was a total of 1.67 mm of surface flow within the observation period between May 21 and July 2 (with a discharge rate of 1.67%) with a total rainfall of 67 mm, and 20.96 g of washed-off soil. The dissolved phase ^{137}Cs and ^{90}Sr activity concentrations were 2.35 and 69.30 Bq L^{-1}, respectively, in the surface runoff. The particulate ^{137}Cs concentration was 322.04 Bq g^{-1}. During the event on June 12, the rainfall occurred between 12:50 and 13:15, and the maximum intensity was 5.6 mm per 5 min. Surface runoff was observed from 13:15 to 13:35, and we also observed a saturated USLE surface (area considered to contribute to surface runoff; Fig. 3). Just after the rainfall began (13:05), no saturated area was observed; however, 10 min later, a saturated area had formed from the bottom to the center of the plot (Fig. 3B). After the rainfall stopped, the saturation zone gradually shrank (Fig. 3C−E) and finally disappeared (Fig. 3F).

A runoff event was also observed on June 30 at the RF site in which rainfall of about 0.2 mm per 5 min was observed intermittently from 3:40. However, no saturated zone was confirmed at 5:35 (Fig. 4A) because of the low intensity of rainfall. A relatively high-rainfall event (2.2 mm per 5 min) began from 5:55, and 10 min later, a small saturation area was observed inside the plot (Fig. 4B). The saturation area then extended from the bottom to the middle of the plot (Fig. 4C and D). Subsequently, a discontinuously saturated area in the lower part of the plot was observed at 7:35 (Fig. 4E), and the saturated area had disappeared by 8:05 with the cessation of rainfall (Fig. 4E). Rainfall also occurred on July 17−28 at the RF site, and a total of 102.4 mm of rainfall gave a surface runoff of 1.68 mm (outflow rate of 1.64%) and 44.81 g of sediment wash-off in total. The dissolved ^{137}Cs and ^{90}Sr concentrations in the surface run-off

Table 2
Summary of observation results of surface wash-off, sediment discharge, and radionuclide activity concentration in the collected samples. Events 1 and 2 in the Red Forest were identified from the 5-min-discharge data at the V-notch weir.

Site	Sampling duration		Event	Rain	R-factor	Discharge		Sediment		Dissolved ^{137}Cs concentration	Solid ^{137}Cs concentration	Dissolved ^{90}Sr concentration
	Start	End		(mm)	(MJ mm ha^{-1} h^{-1})	(mm)	(%)	(g L^{-1})	(g)	(Bq L^{-1})	(Bq g^{-1})	(Bq L^{-1})
Red Forest	2018/6/12 12:50	2018/6/30 10:05	–	67.6	214.3	1.13	1.67	0.17	20.96	2.35	322.04	69.3
	2018/6/12 12:50	2018/6/12 13:40	Event 1	10.2	17.1	0.71	–	–	–	–	–	–
	2018/6/30 3:45	2018/6/30 10:05	Event 2	57.4	197.2	0.42	–	–	–	–	–	–
	2018/7/17 7:10	2018/7/28 7:20	–	102.4	43.2	1.68	1.64	0.24	44.81	1.34	246.66	80.5
Kopachi	2018/6/30 3:35	2018/6/30 14:55	–	41.6	126.6	0.67	1.62	0.23	17.11	9.26	55.82	67.05

Fig. 3. Surface wash-off event on June 12, 2018 at the Red Forest (post-fire) site. The dashed line shows the saturated surface areas, which were detected with the interval camera. (For interpretation of the references to colour in this figure legend, the reader is referred to the Web version of this article.)

were 1.34 and 80.50 Bq L^{-1}, respectively. The particulate ^{137}Cs concentration was 246.66 Bq g^{-1} (Table 2).

In the case of the KP site, we observed surface runoff on June 30, during the observation period from May 21 to July 2. The total surface runoff was 0.67 mm (runoff rate was 1.62% for 41.6 mm of rainfall), and we observed 55.82 g suspended sediment in the wash-off. The dissolved ^{137}Cs and ^{90}Sr concentrations in the surface runoff were 9.26 and 67.05 Bq L^{-1}, respectively. The particulate ^{137}Cs concentration was 55.82 Bq g^{-1} in the suspended sediment. Although the ground surface condition was also observed with the interval camera at the KP site, it is not shown because the ground surface was covered with understory vegetation and litter.

3.2. Surface wash-off and radionuclide fluxes

We next summarize the accumulated rainfall, surface runoff and radionuclide fluxes in the dissolved and particulate form during the summer (May–September) in 2018 (Table 3). The rainfall and surface runoff were 285.8 and 2.81 mm, respectively. Dissolved wash-off of ^{137}Cs and ^{90}Sr was 4.90 and 213.56 Bq m^{-2}, respectively, and particulate wash-off of ^{137}Cs was 160.90 Bq m^{-2} at the RF site. At the KP site, rainfall and surface runoff were 182.2 and 0.67 mm, respectively. Dissolved wash-off of ^{137}Cs and ^{90}Sr was 6.22 and 45.08 Bq m^{-2}, respectively, and particulate wash-off of ^{137}Cs was 8.63 Bq m^{-2}. It should be noted that the 44 rainy days were
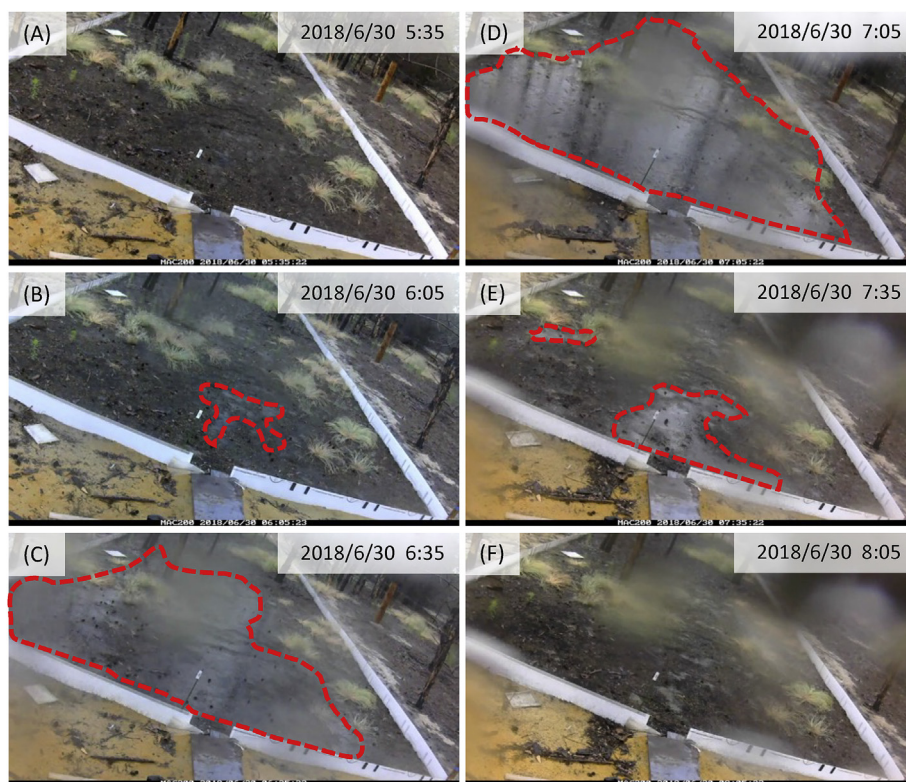
Fig. 4. Surface wash-off event on June 30, 2018 at the Red Forest (post-fire) site. The dashed line shows the saturated surface areas, which were detected with the interval camera. (For interpretation of the references to colour in this figure legend, the reader is referred to the Web version of this article.)

Table 3
Summary of summer (May–September 2018) discharge and radionuclide wash-off. The rainfall amount was calculated from May–September rainfall data.

Site	Rainfall	Surface runoff	Dissolved phase ^{137}Cs wash-off	Solid ^{137}Cs wash-off	Dissolved phase ^{90}Sr wash-off
	(mm)	(mm)	(Bq m^{-2})	(Bq m^{-2})	(Bq m^{-2})
Red forest	285.8	2.81	4.9	160.9	213.6
Kopachi	182.2	0.67	6.2	8.6	45.1

observed during the 154-day field observation period (from May to September) in 2018. However, the strong rainfall days (e.g., >10 mm day^{-1}) were limited (18% of total rainy days), and led to two wash-off events at RF, and one wash-off event at KP. Thus, there is an urgent need to further examine hydrological processes such as the rainfall–infiltration relationship, surface runoff and soil erosion to better understand radionuclide redistribution following wildfire in this region.

In general, the smaller amount of accumulated rainfall at KP than at RF was likely to be related to interception of water by the forest canopy at KP. Actually, observed rainfall at the KP site was about 64% of that at the RF site. Previous studies have shown an 18.8%–45% interception rate in temperate coniferous forests (Alavi et al., 2001; Link et al., 2004; Pypker et al., 2005; Reid and Lewis, 2009) and our results were in agreement with those studies. Furthermore, it is also known that the canopy interruption rate changes with rainfall pattern, for instance, low intensity rainfall has a relatively high interception rate (Carlyle-Moses and Gash, 2011). Thus, we expected that the small interception rate at RF would be important when we evaluated the total flux of water, suspended sediments, and radionuclides.

The slope angle of the USLE could affect the difference between the fluxes between RF and KP. The slope steepness factor (*S*: unitless) (e.g., Benavidez et al., 2018) was calculated from the slope

angle at both sites, and was estimated to be 0.42 and 0.70 for RF and KP, respectively. If the RF had a similar slope to KP, the water, suspended sediments, and radionuclides could be expected to increase about 1.7 times according to the USLE equation. Furthermore, in the case of steep terrain such as Japan's forest area (for example, 27.5° (*S* = 7.25); Yoshimura et al., 2015a), it was assumed that the fluxes would be 17.3 times higher than RF. Therefore, further surface runoff and radionuclide wash-off would be expected if the wildfires occurred on steep slopes. In addition, the wildfires in 2016 occurred distant from the river network (Fig. 1D). If the wildfire occurred near the river network, it can be assumed that the surface runoff and radionuclide wash-off might connect the river water system directly. As a result, the wildfires could be considered to enhance ^{90}Sr mobility and increase the ^{90}Sr flux in the river water system of the CEZ.

3.3. Dissolved-particulate distribution and wash-off coefficients

The dissolved-particulate distribution coefficients (K_d) and normalized dissolved and particulate wash-off coefficients (N_l and N_s) were useful for describing the characteristics of dissolved and particulate radionuclide wash-off (Table 4). In 2018, K_d in RF was 30 times higher than that in KP. This indicates that the particulate ^{137}Cs concentration was much higher than the dissolved ^{137}Cs

Table 4
Normalized wash-off coefficients (N_l and N_s) for ^{137}Cs and ^{90}Sr and solid−liquid distribution coefficient (K_d) in surface runoff based on experiments and field observations on runoff plots.

Site	Period	Land use	N_l (^{137}Cs) (m^{-1})	N_s (^{137}Cs) (m^2 g^{-1})	N_l (^{90}Sr) (m^{-1})	K_d (^{137}Cs) (L kg^{-1})	Reference	Note
Red Forest	2018	Post wildfire	1.18E−05	2.17E−06	6.35E−03	1.84 E+05	This study	Standard USLE
Kopachi	2018	Forest	1.06E−03	6.42E−06	1.07E−02	6.03 E+03		runoff plots
Kopachi	1987	Forest	5.7E−02	3.2E−04	6.6E−02	5.6 E+03	Borzilov et al. (1988)	
Fukushima, Kawamata	2012	Farmland A1 (Uncultivated)	–	4.28E−05	–	–	Yoshimura et al. (2015a)	Standard USLE
	2012	Farmland A2 (Cultivated)	–	1.05E−05	–	–		runoff plots
	2012	Farmland B1 (Uncultivated)	–	5.25E−05	–	–		
	2012	Farmland B2 (Cultivated)	–	3.82E−06	–	–		
	2012	Grassland A	–	2.14E−05	–	–		
	2012	Grassland B	–	9.72E−06	–	–		
	2012	Forest	–	8.17E−05	–	–		
Chernobyl zone. Heavy rain experiment	1986	Abandoned meadow farmland, grassland, and forest	4.49E−02	2.08E−04	1.48E−01	4.62 E+00	Garcia-Sanchez et al. (2005)	1 m × 1 m erosion plot
	1987		1.24E−03	6.83E−05	9.02E−02	5.52 E+01		
	1988		1.31E−02	9.91E−05	1.14E−01	7.56 E+00		
	1989		1.16E−02	4.87E−04	2.82E−01	4.19 E+01		
	1990		–	–	5.17E−01	–		
	1991		1.20E−02	4.58E−05	2.43E−02	3.83 E+00		
Chernobyl, Dovlyady	1986		1.47E−02	1.52E−04	1.00E−01	1.03 E+01	Bulgakov et al. (1991)	1 m × 1 m erosion plot
Chernobyl	1988		2.50E−03	–	2.40E−02	–	Bulgakov et al. (1999)	1 m × 1 m erosion plot
	1988		–	–	1.80E−02	–		

concentration, suggesting that the ^{137}Cs in washed-off ash was less soluble than that of sediment in the water. Further research into the sorption and fixation of radiocesium in the ash is needed to improve understanding of the dissolved particulate distribution. The higher K_d at the RF site than at KP suggests the importance of particulate ^{137}Cs wash-off from the post-fire site in the CEZ, and ^{137}Cs from the wash-off sediment and ash behavior in the river system. Thus, further studies on particulate ^{137}Cs wash-off are also needed.

The entrainment coefficient for dissolved ^{137}Cs concentrations (N_l (^{137}Cs)) were about −3 orders of magnitude at the KP site. The N_l (^{137}Cs) values were about 1 order of magnitude (53 times) lower than the result obtained at the same place in the CEZ immediately after the accident (Borzilov et al., 1988). These findings suggest that the transition from soil to surface flow was greatly reduced over time (Konoplev et al., 1992; Smith et al., 1995; Smith et al., 2000). It is thought that this is because of downward penetration to deeper soil; however, N_l (^{137}Cs) showed little change up to about 5 years after the accident (Bulgakov et al., 1991; Bulgakov et al., 1999; Garcia-Sanchez et al., 2005). Here, N_s (^{137}Cs) was also about 1 order (50 times) smaller than that found in the previous study (Borzilov et al., 1988). In principle, the value of N_s (^{137}Cs) should be decreased by the effect of the downward migration of the ^{137}Cs from shallow soil to deeper soil over time. Actually, the ^{137}Cs concentration was shown to increase with depth in the current study (Table 1). Thus, we suggest that the reduction of N_s (^{137}Cs) during the 30 years since the accident may be attributed to the decrease in the surface layer ^{137}Cs concentration because of downward migration.

Interestingly, K_d, which is defined by the dissolved-particulate distribution, at the KP site was similar between the 1987 experiment (Borzilov et al., 1988) and the current study. This result suggests that the fixation-remobilization fraction (leaching-sorption speed) (Konoplev et al., 1992; Konoplev and Bulgakov, 2000a) had not changed during the 30 years since the CNPP accident.

The entrainment coefficient for dissolved strontium (N_l (^{90}Sr)) also decreased. The N_l (^{90}Sr), which is known as a high-mobility radionuclide (Konoplev et al., 1992), was thus expected to rapidly reduce, but the reduction of was about 6 times smaller than that of N_l (^{137}Cs) during the 30 years. It has been previously pointed out

that ^{90}Sr, which has a higher mobility than that of ^{137}Cs in terms of biomass uptake, was released in litter fall (Thiry et al., 2009). Therefore, it was assumed that the direct leaching from the litter layer, which showed a high ^{90}Sr concentration (Table 1), could contribute toward the small N_l (^{90}Sr) value compared with that of N_l (^{137}Cs).

4. Conclusions

This is the first study to examine the radionuclide wash-off following wildfire within the Chernobyl exclusion zone. We monitored the surface runoff and the radionuclide wash-off using soil erosion plots throughout the summer in 2018. At the post-fire site, 2.81 mm surface runoff was observed after a rainfall event (total amount 285.8 mm). As a result, the dissolved and solid ^{137}Cs fluxes were observed as 4.90 and 160.90 Bq m^{-2}, respectively, and the dissolved ^{90}Sr flux was estimated as 213.56 Bq m^{-2}. At the forest site, in contrast, a single surface runoff (0.67 mm) was generated by a 182.2 mm rainfall event. As a result, the dissolved and solid ^{137}Cs fluxes were observed as 6.22 and 8.63 Bq m^{-2}, respectively, and the dissolved ^{90}Sr flux was 45.08 Bq m^{-2}. In 2018, the distribution coefficient, which is defined by the dissolved-particulate distribution, in the post-fire site, was 30 times higher than that in the forest site, indicating the importance of particulate ^{137}Cs wash-off after fire areas in the Chernobyl exclusion zone. The entrainment coefficient for dissolved and particulate ^{137}Cs concentrations were around 50 times lower than the results obtained in the corresponding position within the Chernobyl exclusion zone immediately after the accident in 1987 (Borzilov et al., 1988). Interestingly, distribution coefficient at the forest site was almost the same in 1987 as found in this study. This suggests that the fixation-remobilization fraction did not change over the 30-year period. However, our results were limited because the field experiment was conducted based on only natural rainfall events. Therefore, there is an urgent need to further examine hydrological processes such as surface runoff and soil erosion, to improve our understanding of radionuclide redistribution following wildfire in the Chernobyl exclusion zone.

Declaration of competing interest

The authors declare no competing interests.

CRediT authorship contribution statement

Yasunori Igarashi: Conceptualization, Formal analysis, Writing - original draft, Writing - review & editing. **Yuichi Onda:** Conceptualization, Formal analysis, Writing - original draft, Writing - review & editing. **Yoshifumi Wakiyama:** Formal analysis, Writing - review & editing. **Alexei Konoplev:** Writing - review & editing. **Mark Zheleznyak:** Writing - review & editing. **Hlib Lisovyi:** Investigation, Methodology. **Gennady Laptev:** Investigation, Methodology. **Volodyill Damiyanovich:** Investigation, Methodology. **Dmitry Samoilov:** Investigation, Methodology. **Kenji Nanba:** Writing - review & editing, Funding acquisition. **Serhii Kirieiev:** Writing - review & editing, Funding acquisition.

Acknowledgements

Appendix A. Supplementary data

Supplementary data to this article can be found online at https://doi.org/10.1016/j.envpol.2019.113764.

References

Alavi, G., Jansson, P.-E., Hällgren, J.-E., Bergholm, J., 2001. Interception of a dense spruce forest, performance of a simplified canopy water balance model. Nord. Hydrol 32, 265—284. https://doi.org/10.2166/nh.2001.0016.

Arkhipov, N.P., Kuchma, N.D., Askbrant, S., Pasternak, P.S., Musica, V.V., 1994. Acute and long-term effects of irradiation on pine (*Pinus silvestris*) stands post-Chernobyl. Sci. Total Environ. 157, 383—386. https://doi.org/10.1016/0048-9697(94)90601-7.

Benavidez, R., Jackson, B., Maxwell, D., Norton, K., 2018. A review of the (Revised) Universal Soil Loss Equation ((R)USLE): with a view to increasing its global applicability and improving soil loss estimates. Hydrol. Earth Syst. Sci. 22, 6059—6086. https://doi.org/10.5194/hess-22-6059-2018.

Borzilov, V.A., Konoplev, A.V., Revina, S.K., 1988. Experimental study of wash-off of radionuclides deposited on soil as result of the accident at Chernobyl Nuclear Power Plant (in Russian). Meteorogiya i Gidrogiya 11, 43—53.

Bugai, D., Dewiere, L., Kashparov, V., Ahamdach, N., 2002. Strontium-90 transport parameters from source term to aquifer in the Chernobyl Pilot site. Radioprotection 37, 11—16.

Bulgakov, A.A., Konoplev, A.V., Popov, V.Y., Shcherbak, A.V., 1991. Removal of long-lived radionuclides from the soil by surface runoff near the Chernobyl Nuclear Power station. Sov. Soil Sci. Pochvovedeniye 23, 124—131.

Bulgakov, A.A., Konoplev, A.V., Shveikin, Y.V., Scherbak, A.V., 1999. Experimental study and prediction of dissolved radionuclide wash-off by surface runoff from non-agricultural watersheds. In: Contaminated Forests. Springer Netherlands, Dordrecht, pp. 103—112. https://doi.org/10.1007/978-94-011-4694-4_11.

Carlyle-Moses, D.E., Gash, J.H.C., 2011. Rainfall interception loss by forest canopies. In: Levia, D.F., Carlyle-Moses, D., Tanaka, T. (Eds.), Forest Hydrology and Biogeochemistry SE - 20, Ecological Studies. Springer Netherlands, pp. 407—423. https://doi.org/10.1007/978-94-007-1363-5_20.

Debano, L.F., Krammes, J.S., 1966. Water repellent soils and their relation to wildfire temperatures. Int. Assoc. Sci. Hydrol. Bull. 11, 14—19. https://doi.org/10.1080/02626666609493457.

Debano, L.F., Osborn, J.F., Krammes, J.S., Leter, J.J., 1967. Soil Wettability and Wetting Agents . . . Our Current Knowledge of the Problem. Berkeley, Calif., Pacific SW. Forest & Range Exp. Sta. U.S. Forest Serv, pp. 1—13. Res. Paper PSW-43.

Evrard, O., Onda, Y., Laceby, J.P., Ayrault, S., Lepage, H., Cerdan, O., 2015. Radiocesium transfer from hillslopes to the pacific ocean after the Fukushima nuclear power plant accident: a review. J. Environ. Radioact. 148, 92—110. https://doi.org/10.1016/j.jenvrad.2015.06.018.

Garcia-Sanchez, L., Konoplev, A., Bulgakov, A., 2005. Radionuclide entrainment coefficients by wash-off derived from plot experiments near chernobyl.

Radioprotection 40, S519—S524. https://doi.org/10.1051/radiopro:2005s1-076.

Garcia-Sanchez, L., Konoplev, A.V., 2009. Watershed wash-off of atmospherically deposited radionuclides: a review of normalized entrainment coefficients. J. Environ. Radioact. 100, 774—778. https://doi.org/10.1016/j.jenvrad.2008.08.005.

Huffman, E.L., MacDonald, L.H., Stednick, J.D., 2001. Strength and persistence of fire-induced soil hydrophobicity under ponderosa and lodgepole pine, Colorado Front range. Hydrol. Process. 15, 2877—2892. https://doi.org/10.1002/hyp.379.

Imeson, A.C., Verstraten, J.M., van Mulligen, E.J., Sevink, J., 1992. The effects of fire and water repellency on infiltration and runoff under Mediterranean type forest. Catena 19, 345—361. https://doi.org/10.1016/0341-8162(92)90008-Y.

Inbar, M., Tamir, M., Wittenberg, L., 1998. Runoff and erosion processes after a forest fire in Mount Carmel, a Mediterranean area. Geomorphology 24, 17—33. https://doi.org/10.1016/S0169-555X(97)00098-6.

International Atomic Energy Agency, 2006. Radiological Conditions in the Dnieper River Basin. Encyclopedia of Atmospheric Sciences.

Iwagami, S., Onda, Y., Tsujimura, M., Abe, Y., 2017. Contribution of radioactive ^{137}Cs discharge by suspended sediment, coarse organic matter, and dissolved fraction from a headwater catchment in Fukushima after the Fukushima Dai-ichi Nuclear Power Plant accident. J. Environ. Radioact. 166, 466—474. https://doi.org/10.1016/j.jenvrad.2016.07.025.

Konoplev, A.V., Bulgakov, A.A., 1995. Modelling of the Transformation of Speciation Processes of Chernobyl Origin Cs-137 and Sr-90 in the Soil and in Bottom Sediments. IAEA SM339.

Konoplev, A.V., Bulgakov, A.A., 1999. Kinetics of the leaching of ^{90}Sr from fuel particles in soil in the near zone of the chernobyl nuclear power plant. At. Energy 86, 136—141. https://doi.org/10.1007/BF02673535.

Konoplev, A.V., Bulgakov, A.A., 2000a. Transformation of the forms of ^{90}Sr and ^{137}Cs in soil and bottom deposits. At. Energy 88, 56—60. https://doi.org/10.1007/BF02673321.

Konoplev, A.V., Bulgakov, A.A., 2000b. Sr-90 and Cs-137 exchange distribution co-efficient in soil—water systems. At. Energy 88, 158—163. https://doi.org/10.1007/BF02673298.

Konoplev, A.V., Bulgakov, A.A., Popov, V.E., Bobovnikova, T.I., 1992. Behaviour of long-lived Chernobyl radionuclides in a soil—water system. Analyst 117, 1041—1047. https://doi.org/10.1039/an9921701041.

Konoplev, A.V., Bulgakov, A.A., Popov, V.E., Popov, O.F., Scherbak, A.V., Shveikin, YuV., Hoffman, F.O., 1996. Model testing using Chernobyl data: I. Wash-off of ^{90}Sr and ^{137}Cs from two experimental plots established in the vicinity of the Chernobyl reactor. Health Phys. 70, 8—12.

Konoplev, A., Golosov, V., Laptev, G., Nanba, K., Onda, Y., Takase, T., Wakiyama, Y., Yoshimura, K., 2016. Behavior of accidently released radiocesium in soil—water environment: looking at Fukushima from a Chernobyl perspective. J. Environ. Radioact. 151, 568—578. https://doi.org/10.1016/j.jenvrad.2015.06.019.

Kutiel, P., Lavee, H., Segev, M., Benyamini, Y., 1995. The effect of fire-induced surface heterogeneity on rainfall-runoff-erosion relationships in an eastern Mediterranean ecosystem, Israel. Catena 25, 77—87. https://doi.org/10.1016/0341-8162(94)00043-E.

Laceby, J.P., Chartin, C., Evrard, O., Onda, Y., Garcia-Sanchez, L., Cerdan, O., 2016. Rainfall erosivity in catchments contaminated with fallout from the Fukushima Daiichi nuclear power plant accident. Hydrol. Earth Syst. Sci. 20, 2467—2482. https://doi.org/10.5194/hess-20-2467-2016.

Link, T.E., Unsworth, M., Marks, D., 2004. The dynamics of rainfall interception by a seasonal temperate rainforest. Agric. For. Meteorol. 124, 171—191. https://doi.org/10.1016/j.agrformet.2004.01.010.

Mills, A., Fey, M., 2004. Frequent fires intensify soil crusting: physicochemical feedback in the pedoderm of long-term burn experiments in South Africa. Geoderma 121, 45—64. https://doi.org/10.1016/j.geoderma.2003.10.004.

Moody, J.A., Shakesby, R.A., Robichaud, P.R., Cannon, S.H., Martin, D.A., 2013. Current research issues related to post-wildfire runoff and erosion processes. Earth Sci. Rev. 122, 10—37. https://doi.org/10.1016/j.earscirev.2013.03.004.

Nagao, S., Kanamori, M., Ochiai, S., Tomihara, S., Fukushi, K., Yamamoto, M., 2013. Export of ^{134}Cs and ^{137}Cs in the Fukushima river systems at heavy rains by typhoon roke in september 2011. Biogeosciences 10, 6215—6223. https://doi.org/10.5194/bg-10-6215-2013.

Nakao, A., Funakawa, S., Takeda, A., Tsukada, H., Kosaki, T., 2012. The distribution coefficient for cesium in different clay fractions in soils developed from granite and paleozoic shales in Japan. Soil Sci. Plant Nutr. 58, 397—403. https://doi.org/10.1080/00380768.2012.698595.

Nakao, A., Ogasawara, S., Sano, O., Ito, T., Yanai, J., 2014. Radiocesium sorption in relation to clay mineralogy of paddy soils in Fukushima, Japan. Sci. Total Environ. 468—469, 523—529. https://doi.org/10.1016/j.scitotenv.2013.08.062.

Nepyivoda, V., 2005. Forestry in the Chornobyl exclusion zone: wrestling with an invisible rival. J. For. 103, 36—40. https://doi.org/10.1093/jof/103.1.36.

Onda, Y., Dietrich, W.E., Booker, F., 2008. Evolution of overland flow after a severe forest fire, Point Reyes, California. Catena 72, 13—20. https://doi.org/10.1016/j.catena.2007.02.003.

Pypker, T.G., Bond, B.J., Link, T.E., Marks, D., Unsworth, M.H., 2005. The importance of canopy structure in controlling the interception loss of rainfall: examples from a young and an old-growth Douglas-fir forest. Agric. For. Meteorol. 130, 113—129. https://doi.org/10.1016/j.agrformet.2005.03.003.

Reid, L.M., Lewis, J., 2009. Rates, timing, and mechanisms of rainfall interception loss in a coastal redwood forest. J. Hydrol. 375, 459—470. https://doi.org/10.1016/j.jhydrol.2009.06.048.

Renard, K.G., Freimund, J.R., 1994. Using monthly precipitation data to estimate the

R-factor in the revised USLE. J. Hydrol. 157, 287—306. https://doi.org/10.1016/0022-1694(94)90110-4.

Robichaud, P.R., 2003. Infiltration rates after prescribed fire in Northern Rocky Mountain forests. In: Soil Water Repellency. Elsevier, pp. 203—211. https://doi.org/10.1016/B978-0-444-51269-7.50021-7.

Sakaguchi, A., Tanaka, K., Iwatani, H., Chiga, H., Fan, Q., Onda, Y., Takahashi, Y., 2015. Size distribution studies of 137 Cs in river water in the abukuma riverine system following the Fukushima dai-ichi nuclear power plant accident. J. Environ. Radioact. 139, 379—389. https://doi.org/10.1016/j.jenvrad.2014.05.011.

Scott, D.F., Van Wyk, D.B., 1990. The effects of wildfire on soil wettability and hydrological behaviour of an afforested catchment. J. Hydrol. 121, 239—256. https://doi.org/10.1016/0022-1694(90)90234-O.

Shahlaee, A.K., Nutter, W.L., Burroughs, E.R., Morris, L.A., 1991. Runoff and sediment production from burned forest sites in the Georgia piedmont. J. Am. Water Resour. Assoc. 27, 485—493. https://doi.org/10.1111/j.1752-1688.1991.tb01449.x.

Smith, J.T., Hilton, J., Comans, R.N.J., 1995. Application of two simple models to the transport of ^{137}Cs in an upland organic catchment. Sci. Total Environ. 168, 57—61. https://doi.org/10.1016/0048-9697(95)04522-3.

Smith, J.T., Clarke, R.T., Saxén, R., 2000. Time-dependent behaviour of radiocaesium: a new method to compare the mobility of weapons test and Chernobyl derived fallout. J. Environ. Radioact. 49, 65—83. https://doi.org/10.1016/S0265-931X(99)00088-0.

Smith, J., Beresford, N.A., 2005. Chernobyl—Catastrophe and Consequences. Springer, Springer Praxis Books. Springer Berlin Heidelberg. https://doi.org/10.1007/3-540-28079-0.

Thiry, Y., Colle, C., Yoschenko, V., Levchuk, S., Van Hees, M., Hurtevent, P., Kashparov, V., 2009. Impact of Scots pine (*Pinus sylvestris* L.) plantings on long term ^{137}Cs and ^{90}Sr recycling from a waste burial site in the Chernobyl Red forest. J. Environ. Radioact. 100, 1062—1068. https://doi.org/10.1016/j.jenvrad.2009.05.003.

Uematsu, S., Smolders, E., Sweeck, L., Wannijn, J., Van Hees, M., Vandenhove, H., 2015. Predicting radiocaesium sorption characteristics with soil chemical properties for Japanese soils. Sci. Total Environ. 524—525, 148—156. https://doi.org/10.1016/j.scitotenv.2015.04.028.

Wakiyama, Y., Onda, Y., Yoshimura, K., Igarashi, Y., Kato, H., 2019. Land use types control solid wash-off rate and entrainment coefficient of Fukushima-derived ^{137}Cs, and their time dependence. J. Environ. Radioact. https://doi.org/10.1016/j.jenvrad.2019.105990, 105990.

Wischmeier, W.H., Smith, D.D., 1978. Predicting Rainfall Erosion Losses: a Guide to Conservation Planning. U.S. Department of Agriculture, Washington, DC.

Yamashiki, Y., Onda, Y., Smith, H.G., Blake, W.H., Wakahara, T., Igarashi, Y., Matsuura, Y., Yoshimura, K., 2014. Initial flux of sediment-associated radiocesium to the ocean from the largest river impacted by Fukushima Daiichi Nuclear Power plant. Sci. Rep. 4, 3714. https://doi.org/10.1038/srep03714.

Yoschenko, V.I., Kashparov, V.A., Protsak, V.P., Lundin, S.M., Levchuk, S.E., Kadygrib, A.M., Zvarich, S.I., Khomutinin, Y.V., Maloshtan, I.M., Lanshin, V.P., Kovtun, M.V., Tschiersch, J., 2006. Resuspension and redistribution of radionuclides during grassland and forest fires in the Chernobyl exclusion zone: part I. Fire experiments. J. Environ. Radioact. 86, 143—163. https://doi.org/10.1016/j.jenvrad.2005.08.003.

Yoschenko, V., Kashparov, V., Levchuk, S., Lundin, S., Protsak, V., Khomutinin, Y., Glukhovsky, O., Maloshtan, I., Tschiersch, J., 2009. Formation of radioactive aerosol particles during the wildland fires in chernobyl zone and their radioecological impact. In: Oughton, D.H., Kashparov, V. (Eds.), Radioactive Particles in the Environment. NATO Science for Peace and Security Series C: Environmental Security. Springer, Dordrecht, pp. 69—89. https://doi.org/10.1007/978-90-481-2949-2_4.

Yoshimura, K., Onda, Y., Kato, H., 2015a. Evaluation of radiocaesium wash-off by soil erosion from various land uses using USLE plots. J. Environ. Radioact. 139, 362—369. https://doi.org/10.1016/j.jenvrad.2014.07.019.

Yoshimura, K., Onda, Y., Sakaguchi, A., Yamamoto, M., Matsuura, Y., 2015b. An extensive study of the concentrations of particulate/dissolved radiocaesium derived from the Fukushima Dai-ichi Nuclear Power Plant accident in various river systems and their relationship with catchment inventory. J. Environ. Radioact. 139, 370—378. https://doi.org/10.1016/j.jenvrad.2014.08.021.